Acidity enhances the formation of a persistent ozonide at aqueous ascorbate/ozone gas interfaces

Shinichi Enami, M. R. Hoffmann, and A. J. Colussi*

W. M. Keck Laboratories, California Institute of Technology, Pasadena, CA 91125

Edited by Barbara J. Finlayson-Pitts, University of California, Irvine, CA, and approved February 28, 2008 (received for review November 13, 2007)

The pulmonary epithelium, like most aerial biosurfaces, is naturally protected against atmospheric ozone (O_3) by fluid films that contain ascorbic acid (AH_2) and related scavengers. This mechanism of protection will fail, however, if specific copollutants redirect AH_2 and O_3(g) to produce species that can transduce oxidative damage to underlying tissues. Here, the possibility that the synergistic adverse health effects of atmospheric O_3(g) and acidic particulate matter revealed by epidemiological studies could be mediated by hitherto unidentified species is investigated by electrospray mass spectrometry of aqueous AH_2 droplets exposed to O_3(g). The products of AH_2 ozonolysis at the relevant air–water interface shift from the innocuous dehydroascorbic acid at biological pH to a C_4-hydroxy acid plus a previously unreported ascorbate ozonide (m/z = 223) below pH ≈5. The structure of this ozonide is confirmed by tandem mass spectrometry and its mechanism of formation delineated by kinetic studies. Present results imply enhanced production of a persistent ozonide in airway-lining fluids acidified by preexisting pathologies or inhaled particulate matter. Ozonides are known to generate cytotoxic free radicals *in vivo* and can, therefore, transduce oxidative damage.

ascorbic acid | oxidative damage | particulate matter | lung | biosurfaces

Epidemiological and toxicological studies show that atmospheric ozone (O_3) and particulate matter (PM) pollutants induce synergistic harmful effects on the health of humans (1–5), animals, and vegetation (6–8). The mechanism by which this synergy operates is, however, unknown. Prompt epithelial damage and inflammation after exposure to these pollutants suggest local rather than systemic action. Because biosurfaces are universally protected by interfacial fluids containing antioxidants such as ascorbic acid (AH_2), reduced glutathione (GSH), and uric acid (UA) in mM concentrations, which intercept and prevent gaseous O_3 from reaching the underlying tissues, a rational approach to unraveling the mechanism of synergic oxidative stress would involve the characterization of chemical events that impair or disable this natural line of defense. The high reactivity of O_3 implies that oxidative aggression is transduced across epithelial lining fluids (ELF) by deleterious secondary oxidants generated in the rapid ozonolysis of sacrificial antioxidants (9–12). These secondary oxidants need only last the few microseconds required for diffusing through typical ≈0.1-μm-thick ELF layers (13). The production of $O_2(^1\Delta_g)$ in high yields (>90%) during the ozonolysis of AH_2 (pK_a = 4.1) in bulk aqueous solution at pH ≈7 (14, 15) implicates the exoergic two-electron oxidation into dehydroascorbic acid (DHA), reaction **1** (16–18):

$$AH^- + O_3 + H^+ \rightarrow DHA + H_2O + O_2(^1\Delta_g) \qquad [1]$$

as the major reaction pathway under physiological conditions. Because superoxide dismutase, catalase, mannitol, and Fe chelators do not inhibit the AH_2-mediated oxidation of red cell membrane proteins, O_2^-, H_2O_2, OH, and Fe–O complexes are unlikely participants in this phenomenon (9). In contrast with reaction **1**, the ozonolysis of unsaturated neutral species, such as undissociated AH_2, in nonaqueous media ultimately produces stable (Criegee or secondary) 1,2,4-trioxolane ozonides (19, 20). In water, however, the dominant products are α-hydroxyalkyl hydroperoxides rather than ozonides (21, 22). Significantly, the $O_2(^1\Delta_g)$ yields and rates of the AH_2, GSH, and UA reactions with O_3(g) measured at the air–water interface are markedly different from those reported in bulk solution (23). Because atmospheric O_3(g) necessarily interacts with biosurfaces through interfacial layers of reduced water activity, the ozonolysis of AH_2 at air/acidic water interfaces could produce ozonides in significant yields. Here, we investigate this possibility in specifically designed laboratory experiments.

The Technique

Our experiments approach the relevant O_3(g)/biosurface interactions in microdroplets generated by spraying aqueous AH_2 solutions into dilute O_3(g)/N_2 mixtures at atmospheric pressure. The composition of the interfacial layers of reacting droplets is directly monitored after submillisecond contact times, τ, by online electrospray mass spectrometry (ESMS) of electrostatically ejected anions (24). The experimental setup has been recently described elsewhere (25). Further details are provided as supporting information (SI) *Text*. Aqueous solutions are pumped into the spraying chamber of the mass spectrometer through a grounded stainless steel needle surrounded by a coaxial sheath issuing nebulizer N_2(g). The large difference between the exit velocities of the liquid jet and nebulizer gas forces the liquid to fragment into fine droplets (26). The spray issuing from a grounded nozzle injector consists of a normal distribution of weakly charged droplets centered at charge zero, as expected from statistical charge separation during the fragmentation of a neutral liquid. It is apparent that this statistical charging process naturally discriminates against the production of highly charged droplets. After leaving the reaction zone, fast solvent evaporation leads to droplet shrinkage and concomitant surface charge crowding. Such droplets become mechanically unstable because electric repulsion eventually overtakes liquid cohesion, triggering the spontaneous shedding of their interfacial films into even smaller droplets. This phenomenon repeats itself until ions are ultimately ejected from last-generation nanodroplets by the large electric fields created thereby (27). These gas-phase ions can then be deflected into the mass spectrometer by applying a suitable electric bias to its inlet port. This analytical technique therefore reports the composition of nanodroplets created out of the interfacial layers of microdroplets that had just reacted with O_3(g). From: (*i*) the short τ <1-ms

Author contributions: A.J.C. designed research; S.E. performed research; M.R.H. contributed new reagents/analytic tools; S.E. and A.J.C. analyzed data; and S.E. and A.J.C. wrote the paper.

The authors declare no conflict of interest.

This article is a PNAS Direct Submission.

Freely available online through the PNAS open access option.

*To whom correspondence should be addressed. E-mail: ajcoluss@caltech.edu.

This article contains supporting information online at www.pnas.org/cgi/content/full/Supplemental0710791105/DCSupplemental.

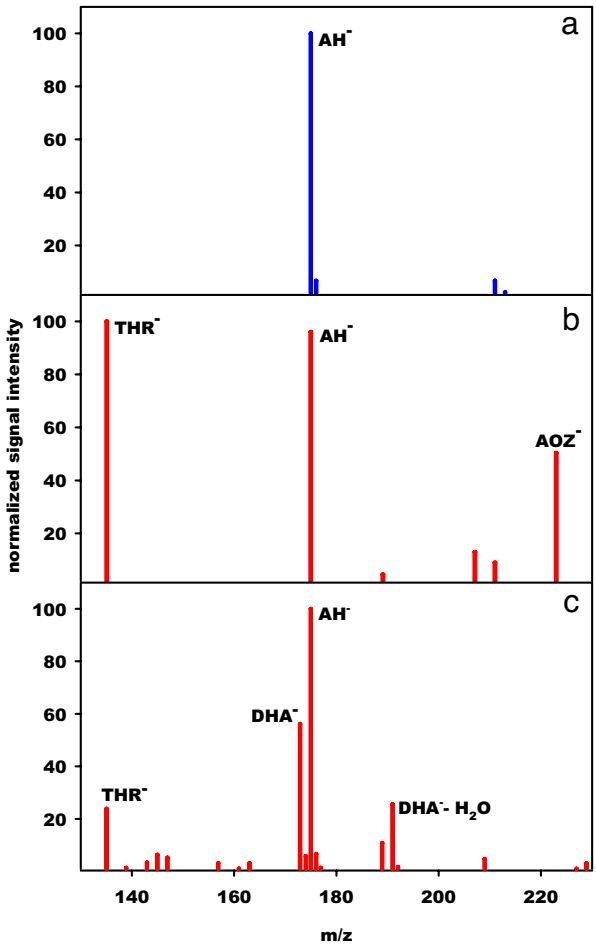

Fig. 1. Negative ion ESMS of aqueous 1 mM L-AH_2 droplets under various conditions: at pH 3.8 in the absence of O_3(g) (*a*), at pH 3.8 in the presence of 1,370 ppm O_3(g) (*b*), and at pH 6.4 in the presence of 1,050 ppm O_3(g) (*c*). The main products of the reaction between AH_2 and O_3(g) at the air–water interface shift from threonate (THR^-) and ascorbate ozonide (AOZ^-) at pH <5, to dehydroascorbate (DHA^-) at pH >6.

contact time, which minimizes the development of secondary chemistry, (*ii*) the demonstrable absence of radical reactions (see below), and (*iii*) the overlapping $[AH^-]/[AH^-]_0$ vs. $[O_3(g)]$ curves in the 10 μM ≤ $[AH^-]_0$ ≤ 1 mM range at pH 3.8 (Fig. S1), we infer that interfacial chemistry is independent of the $[AH_2]/[O_3(g)]$ ratio below ≈10 ppm O_3(g). Therefore, it can be objectively assumed that reactant conversions are proportional to $\tau \times [O_3(g)]$, i.e., that similar conversions are expected at {τ = 1 ms; $[O_3(g)]$ = 100 ppm} and {τ = 1 s; $[O_3(g)]$ = 100 ppb}. Because the numbers of O_3 molecules required to oxidize the same fraction of AH_2 molecules in 10 μM and 1 mM droplets are vastly different, the results of Fig. S1 show that the mass uptake coefficient of O_3(g) is a linearly increasing function of $[AH_2]$, i.e., that the (AH_2 + O_3) reaction is competing with O_3 desorption at the droplet–air interface.

Results

Negative ion ESMS spectra of 1 mM AH_2 solutions display a single signal at m/z = 175 (AH^-) in the 2.4 ≤ pH ≤ 9.0 range (Fig. 1*a*), whose absolute intensity decreases upon O_3(g) injection into the spraying chamber. Below pH ≈5, major signals appear at m/z = 135 and 223 (Fig. 1*b*), which correspond to threonate (THR^-, 2,3,4-trihydroxy butanoate) and an ascorbate ozonide ($AH^-{\cdot}O_3 \equiv AOZ^-$), respectively. At higher pH, THR^- and AOZ^- signal intensities decline in favor of those of DHA^- (m/z = 173) ([4-C]-H in DHA is acidic: pK_1 ≈8) (17) and its *gem*-diol monohydrate (m/z = 191) (Fig. 1*c*). OH-radicals should not be significantly involved in these experiments because neither the products nor their relative yields change upon addition of up to 100 mM *t*-butanol (28).

Tandem mass spectrometry (MS/MS) of the ascorbate ozonide AOZ^- reveals the onset of collisionally induced dissociation (CID) above an accelerating voltage of 1.00 V into m/z = 135 and 189 daughter ions, associated with $2CO_2$ (−88 Da) and H_2O_2 (−34 Da) neutral losses, respectively. As a direct precedent, the major decomposition channel of the secondary endo-ozonide of limonene, unique among those of substituted cyclohexenes, also involves H_2O_2 extrusion (29). Ozonolysis of L-[3-^{13}C] AH_2 exclusively yields ^{13}C-labeled THR^- (m/z = 136), whereas its [1-^{13}C] and [2-^{13}C] isotopologues exclusively yield unlabeled THR^-, as expected from the decomposition of an asymmetric primary ozonide precursor (POZ in Scheme 1) (19). CID of DHA^- (m/z = 173) yields a m/z = 143 anion from the loss of a neutral HCHO (−30 Da) fragment. The finding that the di-keto form of DHA^- (m/z = 173) is the dominant species in the *in situ* ozonolysis of aqueous AH_2 microdroplets, whereas the ESMS of aqueous DHA solutions exclusively displays the mono- $(DHA{\cdot}H_2O)^-$ (m/z = 191) and di-*gem*-diol hydrates

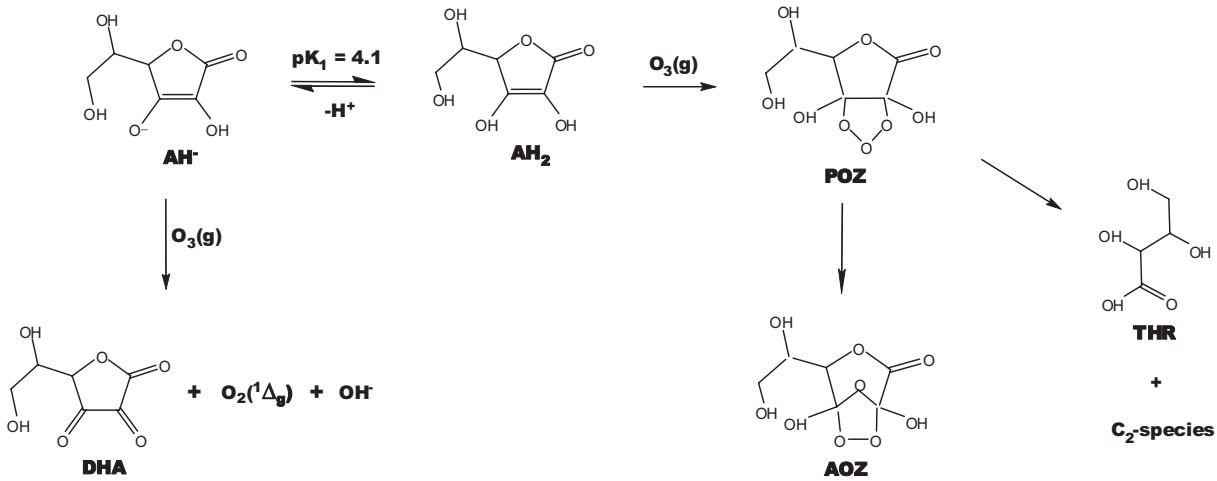

Scheme 1. AH_2 and AH^- reactions with O_3(g) at the air–water interface. DHA is produced directly, whereas THR and the secondary AOZ are formed via an unstable primary 1,2,3-trioxolane ozonide (POZ) (19).

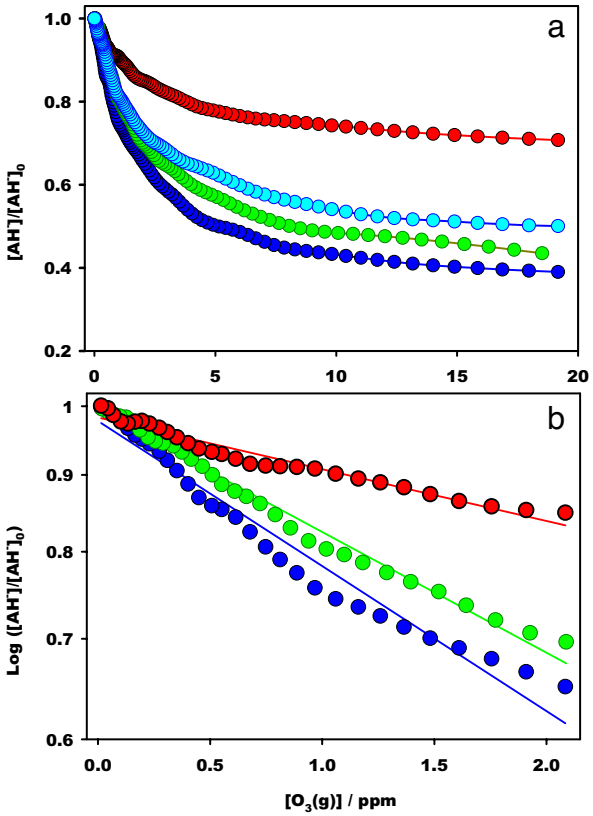

Fig. 2. Normalized ascorbate (m/z = 175) signal intensities in the ozonolysis of 1 mM L-AH_2 by O_3(g) at the air–water interface as functions of [O_3(g)] at various pH values: 3.8 (red), 4.7 (light blue), 5.8 (green), and 8.1 (blue). Symbols are experimental data; lines drawn are visual guides. *b* is a semilog plot of the [O_3(g)] < 2 ppm range of *a*.

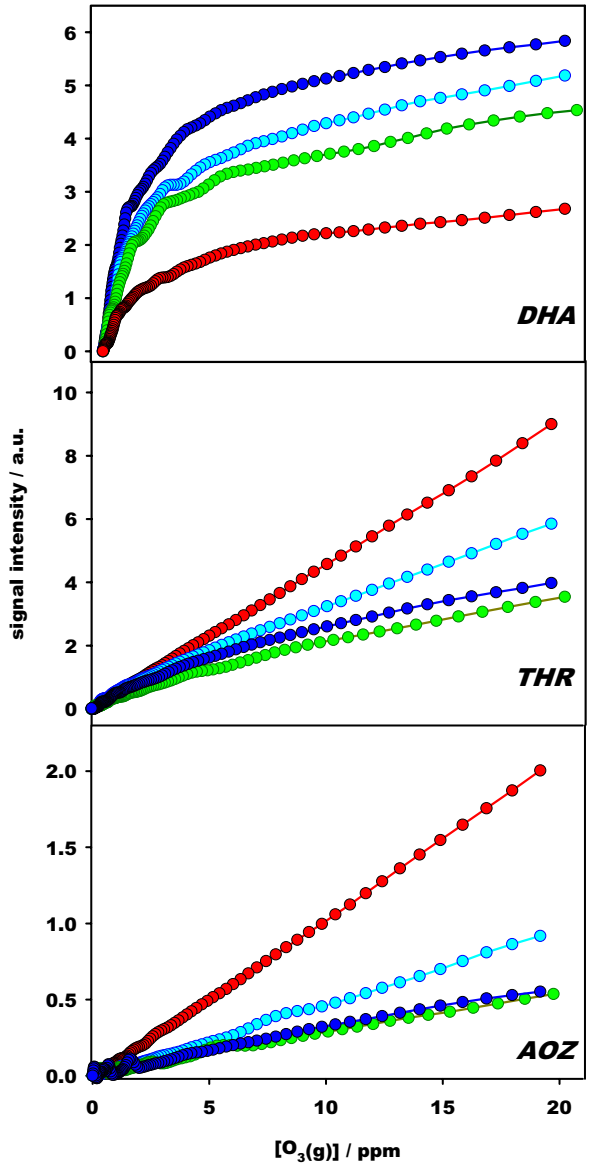

Fig. 3. Products (THR ≡ threonic acid; AOZ ≡ secondary ascorbic acid ozonide, DHA ≡ dehydroascorbic acid) of the reaction between aqueous 1 mM L-AH_2 and O_3(g) at the air–water interface as functions of [O_3(g)] at various pH values: 3.8 (red), 4.7 (light blue), 5.8 (green), and 8.1 (blue). Symbols are experimental data; lines drawn are visual guides. (See Table S2.)

$[DHA{\cdot}(H_2O)_2]^-$ (m/z = 209) indicates incomplete hydration of nascent DHA^- due to kinetic limitations and/or to reduced water availability at the air–water interface. Further evidence that air-solution interfaces are concentrated media is provided by the fact that ESMS signal intensities for anions with large propensities for the air–water interface, such as I^-, plateau above ≈1 mM (30). This is not the case of AH^-, whose ESMS signals increase linearly with [AH^-] in the concentration range used in this work. Remarkably, AOZ^- (m/z = 223) is conspicuously absent from the products obtained by mixing aqueous AH_2 and O_3 solutions before ESMS analysis (Fig. S2 *A* and *B*). The implications are that AOZ^- is formed only at the water-deficient air–water interface, or that its lifetime in bulk water is considerably shorter than the ≈4-s delay between its formation by mixing and ESMS detection. The thermal stability of secondary ozonides favors the former possibility (31–33). Ozone-alkene reactions in dry polluted atmospheres produce stable secondary ozonides (33).

Fig. 2 shows the concentrations of interfacial AH^- after exposure to up to 20 ppm O_3(g) for τ ≈1 ms at various bulk acidities covering the range 3.8 ≤ pH ≤ 8.1. It is apparent that ozonolysis is strongly inhibited at lower pH and that the decline is steeper within pH 3 and 5, as expected from the participation, albeit with different reactivities, of AH_2 and AH^- in this process. Because [AH^-] decreases by ≈50% after exposure to [O_3(g)] < 5 ppm for ≈1 ms at pH >5, AH^- is reacting with an apparent pseudo first-order rate constant: $k^I \approx 10^3\ s^{-1}$, that is much larger that the $k^I \approx 3\ s^{-1}$ value calculated from the reaction rate constant in bulk solution, $k^{II}(AH^- + O_3)_{aq} = 6 \times 10^7\ M^{-1}\ s^{-1}$ (15) and [O_3(aq)] ≈50 nM in water saturated with 5 ppm O_3(g) at 298 K (25). The fact that the depletion of interfacial AH^- levels off above ≈10 ppm O_3(g) is ascribed to efficient reactant influx from the droplets core (see *Appendix 1* in *SI Text* and Fig. S3) rather than to O_3(g) deficiency at the interface, because this phenomenon is common to experiments involving a 100-fold variation of $[AH_2]_0$ (Fig. S1). In *Appendix 1* in *SI Text*, we also show that initial slopes $\gamma = (\partial[AH^-]/\partial[O_3(g)])_{[O3]\to 0}$ in Fig. 2 are proportional to reaction rate constants. In *Appendix 2* in *SI Text*, we evaluate γ (Table S1) and plot them as function of pH in Fig. S4. We find that interfacial γs drop with acidity: γ(pH >7)/γ(pH <3) = 2.73 to a much smaller extent than rate constants for the [AH_2(aq) + O_3(aq)] reaction, k_B, in bulk water: k_B(pH >7)/k_B(pH <3) ≈ 1,600 (15). Together, these findings suggest that the chemical processes we monitor take place in a medium quite different from bulk water, which we ascribe to air–water interfacial layers a few nanometers thick (30).

Fig. 3 shows how pH influences the yields of the products of

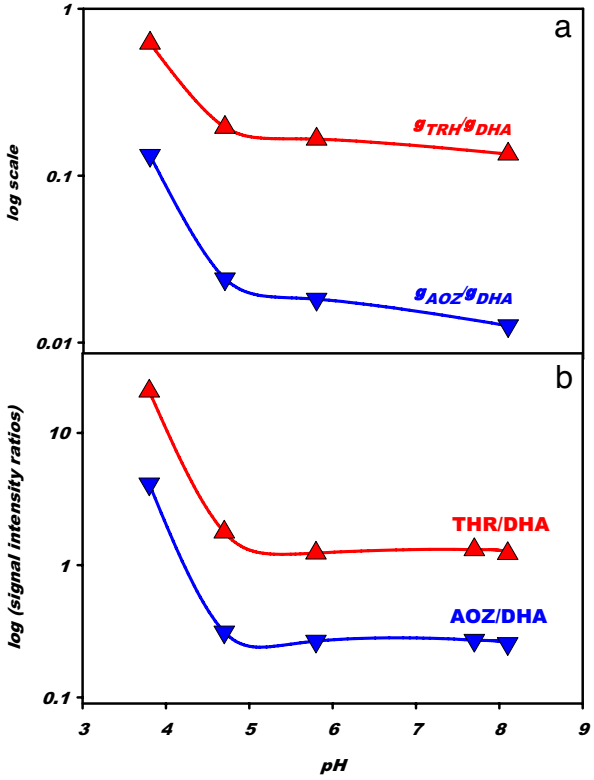

Fig. 4. Product ratios in the interfacial ozonolysis of ascorbate. (*a*) Ratios of initial slopes $\gamma_{THR}/\gamma_{DHA}$ and $\gamma_{AOZ}/\gamma_{DHA}$ for the production of threonic acid (THR), secondary ascorbate ozonide (AOZ), and DHA in 1 mM L-AH_2 exposed to O_3(g) as functions of bulk pH. Lines drawn are visual aids. (See *Appendix 3* in *SI Text* for details.) (*b*) Ratios of ESMS signal intensities THR/DHA and AOZ/DHA in 1 mM L-AH_2 exposed to 800 ppm O_3(g) as functions of bulk pH. Lines drawn are visual aids.

interfacial AH_2 ozonolysis. The formation of DHA^-, the main product above pH ≈6, is appreciably inhibited, whereas THR^- and AOZ^- are enhanced, at lower pH. In *Appendix 3* in *SI Text*, we evaluate the initial slopes of products formation, $\gamma_P = (\partial[P]/\partial[O_3(g)])_{[O3]\to 0}$, from the data of Fig. 3. The calculated $\gamma_{THR}/\gamma_{DHA}$ and $\gamma_{AOZ}/\gamma_{DHA}$ ratios are plotted as functions of pH in Fig. 4*a*. $\gamma_{THR}/\gamma_{DHA}$ and $\gamma_{AOZ}/\gamma_{DHA}$ increase 4.6 and 10.5 times from pH 8.1 to 3.8, respectively. A key clue to the mechanism of reaction is the fact that DHA^- is produced concomitantly with AH^- decay, whereas THR^- and AOZ^- reach limiting yields at much larger [O_3(g)] (Fig. S5). The latter observation shows that DHA^-, AOZ^-, and THR^- are inert toward O_3(g). We infer that DHA^- is produced directly via reaction **1** and that THR^- and AOZ^- are formed in the protracted decomposition of a ESMS-silent intermediate, likely a primary 1,2,3-trioxolane ozonide (POZ) (19). The small kinetic H-isotope effects observed in experiments carried out in H_2O or D_2O solutions (Fig. S6) reveal that none of the rate-controlling steps of the interfacial ozonolysis of aqueous AH_2/AH^- involves significant H-bond forming or breaking.

Discussion

The preceding results and considerations are summarized in Scheme 1. Reaction **1**, with $E^0[O_3(g) + 2H^+ + 2e^- = O_2(^1\Delta_g) + H_2O] = 0.66$ V, $E^0[AH^- = DHA + H^+ + 2e^-] = -0.07$ V at pH 7 (17, 34), is sufficiently exoergic to generate $O_2(^1\Delta_g)$ in high yields. An alternative mechanism initiated by the one-electron transfer reaction: $AH^- + O_3(g) = AH + O_3^-$; $\Delta G^0 = -20$ kJ mol^{-1} (16, 17) should make, at most, a minor contribution to AH_2 ozonolysis because the putative source of $O_2(^1\Delta_g)$, $O_3^- + H^+ = OH + O_2(^1\Delta_g)$; $\Delta G^0 = 66$ kJ mol^{-1} at pH 7 (16, 34), is thermodynamically disallowed and yields OH radicals that should have perceptibly influenced our experiments. O_3 addition to the C=C bond of AH_2 is expected to generate an unstable primary ozonide $AH_2{\cdot}O_3$ (POZ) that will open up to a Criegee diradical intermediate (CI, not shown in Scheme 1), followed by ring reclosure into a secondary ozonide, AOZ, plus typical ozonolysis products resulting from CI fragmentation (19). By assuming a universal neutralization rate constant value of $k^{II}(X^- + H^+)_{aq} \approx 1 \times 10^{10}$ M^{-1} s^{-1}, rate constants for the reverse acid dissociations become: $k^I(XH \to X^- + H^+) \approx 10^{10\text{-}pK_a}$ s^{-1}. Thus, nascent acids weaker than $pK_a \approx 7$ will not dissociate appreciably within the $\tau \approx$1-ms timeframe of our experiments. The primary neutral ozonide POZ, in which the resonance stabilization gained by the ascorbate anion is disrupted, should be a much weaker acid than AH_2. The apparent lack of mass balance in Fig. 3, is ascribed, therefore, to the participation of an unstable, undisssociated POZ intermediate under present conditions. The products of POZ decomposition, threonic acid THR ($pK \approx 3.5$) and the secondary ozonide AOZ, in which 3-C is bonded to three O-atoms are, in contrast, stronger acids that will be readily available as their conjugate anions upon formation. In *Appendix 4* in *SI Text*, we show that the relatively slow (in the millisecond time scale) unimolecular decomposition of POZ into THR and AOZ accounts for nonvanishing γ_{AOZ} (Figs. S7 and S8 *Lower*) and γ_{THR} slopes, but the enhanced production of AOZ and THR at larger [O_3(g)] implies that POZ decomposition is accelerated by O_3 (33). Neither pathway alone is able to account for both nonvanishing initial slopes γ_{AOZ} and increased AOZ production at larger [O_3(g)]. At the [O_3(g)] <0.5 ppm concentrations prevalent in polluted atmospheres, POZ decomposition will proceed unimolecularly in less than ≈1 s. Therefore, the relative amounts of THR/DHA and AOZ/DHA produced at 800 ppm [O_3(g)] in <1 ms vs. pH (Fig. 4*b*) are considered to be more representative of relative product yield dependences on pH under ambient conditions and normal inhalation–exhalation times.

Implications

A persistent ozonide AOZ is therefore produced in larger yields at higher acidities during the ozonolysis of ascorbate at the air–water interface. AOZ may qualify as the stealthy secondary oxidant that diffuses through the ELF toward the biomembranes and trigger inflammatory responses (9). The implication is that AH_2, an otherwise efficient O_3(g) scavenger under normal physiological conditions, should gradually lose its effectivity in ELF that become locally acidified by simultaneous inhalation of acidic airborne particles (35–37) or by preexistent pathologies such as asthma (38) or defective airway pH homeostasis (39). Secondary fine particulate matter ($PM_{<2.5}$) should be particularly detrimental (2) because, by growing on sulfate/sulfuric acid nuclei, is essentially acidic and, because of its small size, can reach deeper into the airways to generate local acidic conditions (39–41). As a reference, the mean pH of exhaled breath condensates in healthy subjects is ≈7.8 but extends down to pH 4.5, particularly in younger individuals (38).

Our findings are relevant to the copollutant dilemma, i.e., the difficulty of parsing the effects of air pollution among PM and non-PM components (37), which remains at the center of current medical, epidemiological, and regulatory debates on tropospheric particulate matter. Should the observed health effects be exclusively ascribed to particulate matter and, if so, to what component(s) of particulate matter, in terms of either particle size or chemistry, or are they elicited by interactions between particulate matter and gaseous copollutants? Epidemiological studies that evaluate associations between biological markers and individual agents, such as ozone, fine particulate matter ($PM_{2.5}$), and iron, are unable to elucidate the causative mech-

anisms (42, 43). The largest pollutant cross-correlations indices, β, ($H^+ + O_3$, $\beta = 0.57$), ($SO_4^{2-} + O_3$, $\beta = 0.66$), and ($PM_{10} + O_3$, $\beta = 0.67$) found in recent time-series analysis of daily mortality and morbidity versus acidic particulate matter data (42) confirm, however, biochemical, toxicological, and morphological studies of lung tissues simultaneously exposed to O_3(g) and acidic (but not neutral) aerosols that revealed strong synergism between these agents (4, 36, 44). The fact that rats exposed in the laboratory to various aerosols, alone or in combination with O_3(g), manifest enhanced oxidative stress upon breathing {O_3(g) + pH $\leqslant$ 4.5 aerosol} mixtures (correlation coefficient 0.98) (36) is consistent with AOZ enhancement below pH 5 (Fig. 4). Secondary ozonides are persistent, strong oxidizers that can actually trigger acute responses *in vivo* (45). Potent synthetic 1,2,4-trioxolane surrogates of the ancient antimalarial drug artemisinin (45–47) have been recently shown to generate cytotoxic carbon-centered radicals in the presence of iron(II) (48). Our work suggests therefore that O_3(g), particle acidity, and quite possibly reduced iron (49) are functionally linked cofactors. Future epidemiological and toxicological studies should address these interesting issues.

ACKNOWLEDGMENTS. We thank C. D. Vecitis and J. Cheng for experimental assistance. S.E. is grateful to Prof. Yutaka Matsumi (Solar–Terrestrial Environment Laboratory, Nagoya University, Nagoya, Japan), Prof. Masahiro Kawasaki (Department of Molecular Engineering, Kyoto University, Kyoto, Japan), and the Japan Society for the Promotion of Science Research Fellowship for Young Scientists. This work was supported by National Science Foundation Grant ATM-0534990.

1. Bosson J, *et al.* (2007) Ozone enhances the airway inflamation initiated by diesel exhaust. *Resp Med* 101:1140–1146.
2. Schlesinger RB (2007) The health impact of common inorganic components of fine particulate matter ($PM_{2.5}$) in ambient air: A critical review. *Inhalation Toxicol* 19:811–832.
3. Borm PJA, Kelly F, Kunzli N, Schins RPF, Donaldson K (2007) Oxidant generation by particulate matter: From biologically effective dose to a promising, novel metric. *Occup Environ Med* 64:73–74.
4. Warren DL, Last JA (1987) Synergistic interaction of ozone and respirable aerosols on rat lungs. 3. Ozone and sulfuric acid aerosol. *Toxicol Appl Pharmacol* 88:203–216.
5. Kleinman MT, Phalen RF (2006) Toxicological interactions in the respiratory system after inhalation of ozone and sulfuric acid aerosol mixtures. *Inhalation Toxicol* 18:295–303.
6. Chameides WL (1989) The chemistry of ozone deposition to plant leaves—Role of ascorbic acid. *Environ Sci Technol* 23:595–600.
7. Cross CE, van der Vliet A, Louie S, Thiele JJ, Halliwell B (1998) Oxidative stress and antioxidants at biosurfaces: Plants, skin, and respiratory tract surfaces. *Environ Health Perspect* 106:1241–1251.
8. Langebartels C, Wohlgemuth H, Kschieschan S, Grun S, Sandermann H (2002) Oxidative burst and cell death in ozone-exposed plants. *Plant Physiol Biochem* 40:567–575.
9. Ballinger CA, *et al.* (2005) Antioxidant-mediated augmentation of ozone-induced membrane oxidation. *Free Radic Biol Med* 38:515–526.
10. Postlethwait EM (2007) Scavenger receptors clear the air. *J Clin Invest* 117:601–604.
11. Pryor WA, *et al.* (2006) Free radical biology and medicine: It's a gas, man! *Am J Physiol* 291:R491–R511.
12. Pryor WA, Squadrito, GL Friedman M (1995) The cascade mechanism to explain ozone toxicity—The role of lipid ozonation products. *Free Radic Biol Med* 19:935–941.
13. Pryor WA (1992) How far does ozone penetrate into the pulmonary air/tissue boundary before it reacts? *Free Radic Biol Med* 12:83–88.
14. Kanofsky JR, Sima P (1991) Singlet oxygen production from the reactions of ozone with biological molecules. *J Biol Chem* 266:9039–9042.
15. Giamalva D, Church DF, Pryor WA (1985) A comparison of the rates of ozonation of biological antioxidants and oleate and linoleate esters. *Biochem Biophys Res Commun* 133:773–779.
16. Bennett LE, Warlop P (1990) Electron-transfer to ozone—Outer-sphere reactivities of the ozone ozonide and related nonmetal redox couples. *Inorg Chem* 29:1975–1981.
17. Creutz C (1981) The complexities of ascorbate as a reducing agent. *Inorg Chem* 20:4449–4452.
18. Koppenol WH (1982) The reduction potential of the couple O_3/O_3^-. *FEBS Lett* 140:169–172.
19. Criegee R (1975) Mechanism of ozonolysis. *Angew Chem Int* 14:745–752.
20. Squadrito G, Uppu RM, Cueto R, Pryor WA (1992) Production of the Criegee ozonide during the ozonation of 1-palmitoyl-2-oleoyl-sn-glycero-3-phosphochloline liposomes. *Lipids* 12:955–958.
21. Gab S, *et al.* (1995) Formation of alkyl and hydroxyalkyl hydroperoxides on ozonolysis in water and in air. *Atmos Environ* 18:2401–2407.
22. Bunnelle WH (1991) Preparation, properties and reactions of carbonyl oxides. *Chem Rev* 91:335–362.
23. Mudway IS, Kelly FJ (1998) Modeling the interactions of ozone with pulmonary epithelial lining fluid antioxidants. *Toxicol Appl Pharmacol* 148:91–100.
24. Kebarle P, Peschke M (2000) On the mechanisms by which the charged droplets produced by electrospray lead to gas phase ions. *Anal Chim Acta* 406:11–35.
25. Enami S, Vecitis CD, Cheng J, Hoffmann MR, Colussi AJ (2007) Global inorganic source of atmospheric bromine. *J Phys Chem A* 111:8749–8752.
26. Manisali I, Chen DDY, Schneider BB (2006) Electrospray ionization source geometry for mass spectrometry: Past, present, and future. *Trends Anal Chem* 25:243–256.
27. Nguyen S, Fenn JB (2007) Gas-phase ions of solute species from charged droplets of solutions. *Proc Natl Acad Sci USA* 104:1111–1117.
28. Flyunt R, *et al.* (2003) Determination of (OH)-O-center dot, O-2(center dot-), and hydroperoxide yields in ozone reactions in aqueous solution. *J Phys Chem B* 107:7242–7253.
29. Nørgaard AW, *et al.* (2006) Secondary limonene endo-ozonide: A major product from gas-phase ozonolysis of R-(+)-limonene at ambient temperature. *Atmos Environ* 40:3460–3466.
30. Cheng J, Vecitis C, Hoffmann MR, Colussi AJ (2006) Experimental anions affinities for the air–water interface. *J Phys Chem B* 110:25598–25602.
31. Perry CS, *et al.* (2006) Chemical kinetics and aqueous degradation pathways of a new class of synthetic ozonide antimalarials. *J Pharm Sci* 95:737–747.
32. Lin AJ, Klayman DL, Hoch JM (1985) Thermal rearrangement and decomposition products of artemisinin (Qinghaosu). *J Org Chem* 50:4504–4508.
33. Karagulian F, Lea SA, Dilbeck CW, Finlayson-Pitts BJ (2008) A new mechanism for ozonolysis of unsaturated organics on solids: phosphocholines on NaCl as a model for sea salt particles. *PhysChemChemPhys* 10:528–541.
34. Bard AJ, Parsons R, Jordan J (1985) *Standard Potentials in Aqueous Solution* (Dekker, New York).
35. Lippmann M (2007) Health effects of airborne particulate matter. *N Engl J Med* 357:2395–2397.
36. Last JA (1991) Global atmospheric change: Potential health effects of acid aerosol and oxidant gas mixtures. *Environ Health Perspect* 96:151–157.
37. Chow JC, *et al.* (2006) Health effects of fine particulate air pollution: Lines that connect. *J Air Waste Manage Assoc* 56:1368–1380.
38. Paget-Brown AO, *et al.* (2006) Normative data for pH of exhaled breath condensate. *Chest* 129:426–430.
39. Ricciardolo FLM, Gaston B, Hunt J (2004) Acid stress in the pathology of asthma. *J Allergy Clin Immunol* 113:610–619.
40. Hunt JF (2006) Exhaled breath condensate pH. Reflecting acidification of the airway at all levels. *Am J Resp Crit Care Med* 173:366–367.
41. Hunt JF (2007) Exhaled breath condensate pH assays. *Immunol Alergy Clin N Am* 27:597–606.
42. Gwynn RC, Burnett RT, Thurston GD (2000) A time–series analysis of acidic particulate matter and daily mortality and morbidity in the Buffalo, New York, region. *Environ Health Perspect* 108:125–133.
43. Pope CA, *et al.* (2004) Ambient particulate air pollution, heart rate variability, and blood markers of inflammation in a panel of elderly subjects. *Environ Health Perspect* 112:339–345.
44. Chen LC, Miller PD, Lam HF, Guty J, Amdur MO (1991) Sulfuric acid-layered ultrafine particles potentiate ozone-induced airway injury. *J Toxicol Environ Health* 34:337–352.
45. Tang YQ, *et al.* (2007) Weak base dispiro-1,2,4-trioxolanes: Potent antimalarial ozonides. *Bioorg Med Chem Lett* 17:1260–1265.
46. Vennerstrom JL, *et al.* (2004) Identification of an antimalarial synthetic trioxolane drug development candidate. *Nature* 430:900–904.
47. Klayman DL (1985) Qinghaosu (Artemisinin): An antimalarial drug from China. *Science* 228:1049–1055.
48. Mercer AE, *et al.* (2007) Evidence for the involvement of carbon-centered radicals in the induction of apoptotic cell death by artemisinin compounds. *J Biol Chem* 282:9372–9382.
49. Ghio AJ, *et al.* (2007) Lung injury after ozone exposure is iron dependent. *Am J Physiol* 292:L134–L143.